Absolute Rotation Angle and Precession Rate of a Traveling Foucault Pendulum

Russell P. Patera[1]

Abstract

The time dependent absolute rotations of the Foucault Pendulum and its mounting fixture were derived for any latitude using attitude kinematics without relying on a detailed solution for the oscillatory motion of the pendulum bob. Employing a novel method to compute the associated solid angle, analytical solutions were found for both rotation angles and their time derivatives, as well as, the associated precession rate. The methodology was extended to a Foucault pendulum traveling across the Earth's surface when the Earth spins at an arbitrary angular rate. When not translating across the Earth's surface, both pendulum and its mounting fixture were found to have absolute rotation rates in the counterclockwise direction in the Northern Hemisphere. The difference in rotation rates is in agreement with the observed relative clockwise precession rate of the pendulum with respect to its mounting fixture. Unlike stationary pendulums, traveling pendulums generally have time varying precession rates. Numerical examples are presented for various cases involving stationary and moving Foucault Pendulums to illustrate the developed methods.

Keywords: Foucault Pendulum, Absolute rotation angle, Precession rate, Attitude kinematics, Slewing transformation, Solid angle

Nomenclature

A	initial axis orientation
a	unit vector of **A**
B	final axis orientation
b	unit vector of **B**
C	axis between **A** and **B**
e, f, d	auxiliary axes
G	auxiliary function
MF	mounting fixture
N	number of steps
P	auxiliary rotation axis
R	slewing axis
R(z, λ)	rotational transformation
S	integral of angular rate about axis **R**
T	total time
t_i	time to the i th time step
U	attitude transformation
$\mathbf{U}_S$	slewing attitude transformation

[1] Russell.P.Patera@gmail.com

$\mathbf{U_{TS}}$	slewing transformation about solid angle region
$\mathbf{U_i}$	transformation to the i th time step
$\mathbf{U_G}$	great circle arc attitude transformation
$\mathbf{U_T}$	total attitude transformation
$\boldsymbol{\omega_P}$	angular rate about axis **P**
$\boldsymbol{\omega_Z}$	angular rate about **z** axis
Ψ	absolute rotation about the mounting fixture vertical axis
λ	Earth rotation angle
Δ	rotational transformation angle
ϕ	external rotation angle associated with solid angle region
σ	rotation angle about axis **P**
Ω	solid angle, absolute rotation about pendulum vertical axis
Γ	axis rotation at vertex of polygon

1. Introduction

The Foucault Pendulum (Sommeria, 2017) is a long spherical pendulum with a significant mass attached to maintain its periodic motion in the presence of frictional forces. The pendulum is mounted to a nearly frictionless bearing to decouple the axial motion about the vertical axis. The motion of the pendulum is initialized such that the pendulum mass moves in a plane containing the vertical axis. The momentum associated with the pendulum's oscillation ensures that its axial rotation is decoupled from the mounting fixture, MF. Once the pendulum begins swinging, the plane of the pendulum's motion appears to rotate or precess about its vertical axis. The precessing Foucault Pendulum was first demonstrated in Paris in 1851 and showed that the Earth rotates (Sommeria, 2017) without relying on a celestial coordinate frame

There are two fundamental approaches to solving the Foucault Pendulum precession problem. The first is dynamical analysis of the pendulum bob and the second is attitude kinematics of the pendulum's vertical axis. Most published analyses involve the dynamical analysis of the pendulum bob, which includes gravitational and tension forces, as well as, centripetal and Coriolis forces that are required when solving the problem in the local non-inertial reference frame. In addition, various assumptions are made, such as, a heavy pendulum bob mass, a long pendulum length and a very small oscillation angle. Dynamical analyses of the motion of the Foucault Pendulum, such as, (Ciureanu and Condurache, 2015), Zhuravlev and Petrov, (2014), Zheng, (2015), and Basano, (2018) have been performed to predict its precession rate for all values of latitude. Since the time scale of the oscillatory motion is much less than the Earth's rotational period, highly accurate methods must be used to extract the very small precession rate. Other researchers found that the precessional motion of the pendulum is the result of geometrical considerations without the use of dynamical analysis (Bergmannn and Bergmann, 2007), (Oprea, 1995).

The second approach to solving the Foucault Pendulum precession problem involves attitude kinematics of the vertical axis of the pendulum, which is fixed to the plane of oscillation of the pendulum. In this approach, the detailed motion of the pendulum bob is not needed, since the pendulum oscillation only serves to ensure that the pendulum is decoupled from the vertical axis rotation of the MF. This realization greatly simplifies the problem, since only the slewing and rotational motions of the pendulum's vertical axis need to be analyzed. A recent work (Patera, 2021) showed that for a complete rotation of the Earth, the precession of the Foucault Pendulum can be explained using Ishlinskii's Theorem in attitude kinematics (Ishlinskii, 1952). Results show that the rotation of the pendulum about its vertical axis is equal to the solid angle of the conical cap north of its latitude, which is $2\pi\,(1-\sin(\Theta))$ radians, where Θ is the latitude. The vertical axis of the pendulum's mounting fixture, MF, has a rotation equal to the pendulum's rotation but with an additional rotation due to the integral of the projection of the Earth's angular rate along the vertical axis, which is $2\pi \sin(\Theta)$ radians. Therefore, for one complete rotation of the Earth, the sum of both rotational contributions indicates that the MF's rotation is 2π radians for any latitude. A more detailed analysis of the pendulum's attitude kinematics (Patera, 2021) was able to quantify the pendulum's motion for Earth rotation angles of less than 2π radians.

The current work is focused on the absolute rotation of the pendulum about its vertical axis rather than its complete attitude motion. Using attitude kinematics, the solid angle associated with the absolute rotation was obtained. A new method to compute the solid angle enabled the derivation of an analytical solution for the pendulum's rotation angle. The pendulum's rotation rate was obtained by differentiating the rotation angle equation. It was found that the pendulum rotates in the counterclockwise direction in the Northern Hemisphere and has a rate that is a nonlinear function of the Earth's rotation angle. The vertical axis of the MF also rotates in the counterclockwise direction but acquires a higher rotation rate than the pendulum due to the contribution from the Earth's spin rate. The difference in the pendulum's rotation rate and the MF's rotation rate accounts for the clockwise precession of the pendulum as observed from the Earth's reference frame.

The general case of a Foucault Pendulum that moves across the Earth's surface with the Earth having an arbitrary angular rate was treated using attitude kinematics. An auxiliary rotation axis was employed to propel the pendulum along the Earth's surface and enable accurate attitude propagation of the pendulum. The results prove that absolute rotation of the pendulum's vertical axis can be created by the slewing motion of the pendulum along the surface of the Earth, even if the Earth is not spinning.

Section 2 contains a derivation of the rotation angle of the Foucault Pendulum's plane of oscillation as a function of Earth rotation angle and latitude. The derivation uses a new method to compute solid angles (Patera, 2020a), which provides an analytical solution. The results are validated with a previously published general method of computing solid angles (Patera, 2020a), (Patera, 2020b). The resulting analytical equation is used to derive the associated rotation angle rate. The same method was used to calculate rotation angle and rate for the MF.

Section 3 contains a derivation of the rotation angle of the Foucault Pendulum's plane of oscillation for the general case of a moving pendulum on the Earth, but with the Earth having arbitrary spin rate. The pendulum's translational motion is driven by a rotation about an auxiliary rotation axis that is fixed in the Earth's reference frame. Thus, the pendulum's translational motion follows a conical trajectory in the Earth relative frame. If the cone angle is 90 degrees the pendulum's trajectory is a great circle arc.

Section 4 contains numerical results that illustrate the pendulum's absolute rotation angle and associated rate for various values of latitude and Earth rotation angle. Results were also obtained for the MF's rotation angle and rate. Both sets of angles and rates indicate nonlinear dependence on the Earth's rotation angle. This feature differs from the pendulum's precession rate, which is a function of latitude but not the Earth's rotation angle.

Section 5 contains numerical results for a moving pendulum with changing latitude and longitude values. Motion of the pendulum along the Earth's surface can result in time varying precession rate. Results for cases involving both spinning and non-spinning Earth are also presented.

Section 6 contains the conclusion.

2. Attitude Kinematics

The rotation of the plane of oscillation of the Foucault Pendulum, which is equivalent to the rotation of the pendulum's vertical axis, is governed by attitude kinematics. Fig. 1 illustrates the pendulum's vertical axis as it slews from orientation **A** to orientation **B** along a conical trajectory with its tip at a fixed value of latitude. It was shown in a recent publication (Patera, 2020a) that the attitude transformation of the axis in going from orientation **A** to orientation **B** along an arbitrary trajectory has three components. The first component of the attitude transformation is the great circle arc transformation linking orientations **A** and **B**. The second component of the attitude transformation is the rotational transformation about the axis at orientation **B** that is equal to the solid angle bounded by the actual trajectory of the axis and the associated great circle arc trajectory. The third component of the attitude transformation is the time integral of the Earth's angular rate along the axis during the slewing motion. Since this work is focused on the rotation about the axis, only the second and third components of the attitude transformation are of concern. The third component of the attitude transformation causes the MF to rotate by an additional amount but does not cause the pendulum to rotate, since the pendulum is decoupled from the MF's vertical axis. Therefore, the pendulum's rotation about its vertical axis is completely determined by the second component of the attitude transformation, which is the solid angle enclosed by the actual trajectory and the great circle arc trajectory.

The general method of computing solid angles, which was presented in an earlier work (Patera, 2020b) can be applied to the Foucault Pendulum. Referring to Fig. 1, the total transformation, **U**, is given by a rotation of λ about the **z**-axis of the Earth, as shown in eq. (1), where **R** is the rotational transformation, **z** is the axis about which the rotation is applied and λ is the magnitude of the rotation angle.

$$\mathbf{U} = \mathbf{R}(\mathbf{z}, \lambda) \tag{1}$$

It was shown in earlier work (Patera, 2021), (Patera, 2020a) that the total transformation is the product of the slewing transformation, $\mathbf{U_S}$, and the rotational transformation, **R**(**B**, Δ), as shown in eq. (2). After the Earth rotates by λ, the axis will have rotated by $\lambda \sin(\Theta)$. Therefore, the angle Δ is given by the integral of the Earth's angular rate along the axis or $\lambda \sin(\Theta)$, where Θ is the latitude. Note that the slewing and rotational transformations commute, as was shown in an earlier work (Patera, 2021), (Patera, 2020a).

$$\mathbf{U} = \mathbf{R}(\mathbf{z}, \lambda) = \mathbf{U_S}\, \mathbf{R}[\mathbf{B}, \Delta] = \mathbf{R}[\mathbf{A}, \Delta]\, \mathbf{U_S} \tag{2}$$

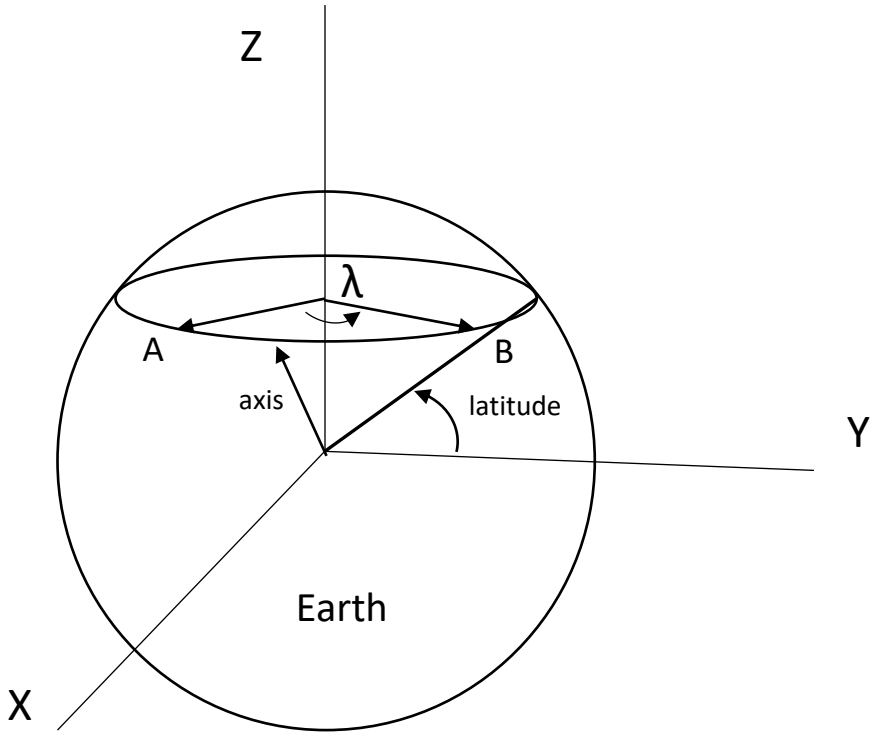

Fig. 1. The pendulum axis moves from orientation **A** to orientation **B** as the Earth rotates by angle λ.

The slewing transformation can be extracted from eq. (2) using the inverse of the respective rotational transformations, as shown in eqs. (3) and (4).

$$\mathbf{U_S} = \mathbf{R}(\mathbf{z}, \lambda)\ \mathbf{R}^{-1}[\mathbf{B}, \lambda \sin(\Theta)] = \mathbf{R}(\mathbf{z}, \lambda)\ \mathbf{R}[\mathbf{B}, -\lambda \sin(\Theta)] \tag{3}$$

$$\mathbf{U_S} = \mathbf{R}^{-1}[\mathbf{A},\ \lambda \sin(\Theta)]\ \mathbf{R}(\mathbf{z}, \lambda) = \mathbf{R}[\mathbf{A}, -\lambda \sin(\Theta)]\ \mathbf{R}(\mathbf{z}, \lambda) \tag{4}$$

The slewing transformations Eqs. (3) and (4) are equal and represent the attitude transformation associated with the slewing motion along the constant latitude arc. The other boundary of the desired solid angle is given by the great circle arc linking orientations **A** and **B**. The great circle arc slewing transformation between orientations **A** and **B** is found using the Pivot Parameter method (Patera, 2017), which involves a sequence of two rotations of 180 degrees about two axes in the slewing plane that are separated by one half the rotation angle. The midpoint orientation of the axis along the great circle arc is needed for the Pivot Parameter method (Patera, 2017). The midpoint orientation is defined by **C** in eq. (5), where **a** and **b** are unit vectors aligned with axes **A** and **B**, respectively.

$$\mathbf{C} = \frac{\mathbf{a}+\mathbf{b}}{|\mathbf{a}+\mathbf{b}|} \tag{5}$$

Using the Pivot Parameter method (Patera, 2017), the slewing transformation along the great circle arc from orientation **B** back to **A**, is given in eq. (6), where the rotation angles are given in degrees.

$$\mathbf{U_G} = \mathbf{R}(\mathbf{B}, 180)\ \mathbf{R}(\mathbf{C}, 180) = \mathbf{R}(\mathbf{C}, 180)\ \mathbf{R}(\mathbf{A}, 180) \tag{6}$$

Therefore, the total slewing transformation around the solid angle region is given by eq. (7), where eqs. (3), (4) and (6) are used for the evaluation in eq. (7).

$$\mathbf{U_{TS}} = \mathbf{U_S}\,\mathbf{U_G} \tag{7}$$

The general method to obtain the solid angle of the region from the slewing transformation about the region was developed in an earlier work (Patera, 2020b). It was found that the solid angle, Ω, is simply the magnitude of the Euler Rotation Vector of the transformation. Therefore, the rotation angle of the pendulum, which is the solid angle of the enclosed region, is given by the magnitude of the Euler Rotation Vector for the transformation $\mathbf{U_{TS}}$, as given in eq. (7).

Although eq. (7) can be used to obtain the rotation angle of the pendulum, a new alternative method (Patera, 2020a) yields an analytical solution that can be used to derive the angular rate of the pendulum. It was shown (Patera, 2020a) that the solid angle of any regular spherical polygon of n sides is given by eq. (8), where ϕ_i are the exterior rotation angles about the vertices made by adjoining adjacent planes. Each of the n sides is a segment of a great circle arc.

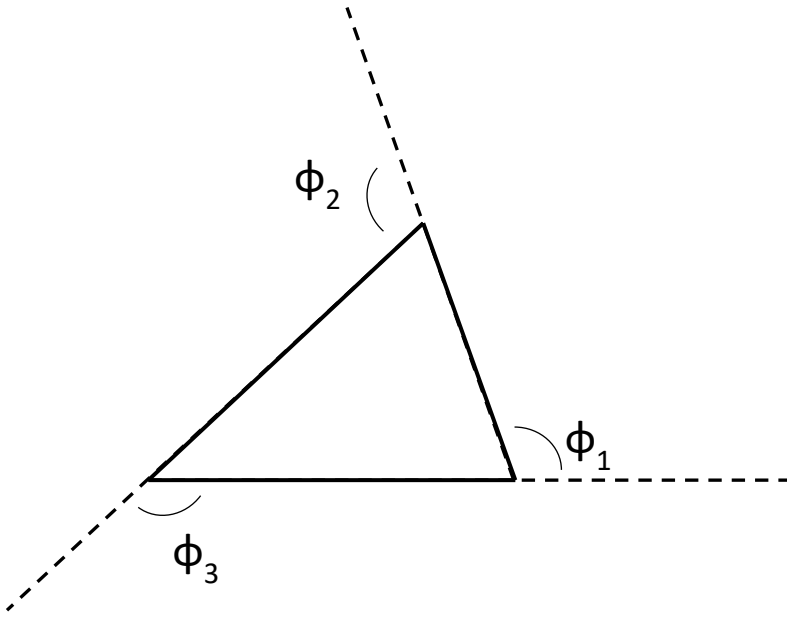

Fig. 2. Exterior angles of a spherical triangle as illustrated on a plane.

Fig. 2 illustrates the case for a spherical triangle as represented on a two dimensional plane. The sum of the exterior angles can be viewed as the rotation of an axis, as the axis moves about the spherical triangle.

$$\Omega = 2\pi - \sum_{i=1}^{n} \phi_i \tag{8}$$

Eq. (8) can be generalized to also include a region of continuous rotation of the axis as it slews about a section of the solid angle region, as shown in eq. (9), where a and b define the region of continuous rotation.

$$\Omega = 2\pi - \sum_{i=1}^{n} \phi_i - \int_a^b d\phi \tag{9}$$

Fig. 3 illustrates the constant latitude slewing trajectory of the pendulum, as well as, the Great Circle arc used to define the solid angle area that quantifies the absolute rotation of the vertical axis of the pendulum. The latitude of the pendulum is indicated by the dashed circular line containing **A** and **B**. The solid circular line defines the equator at 0 deg. latitude. As the Earth spins, the pendulum moves from point **A** to point **B** along a constant latitude trajectory. The dashed line from **B** back to **A** is the great circle arc trajectory, which is used to define the solid angle region needed for the absolute rotation computation.

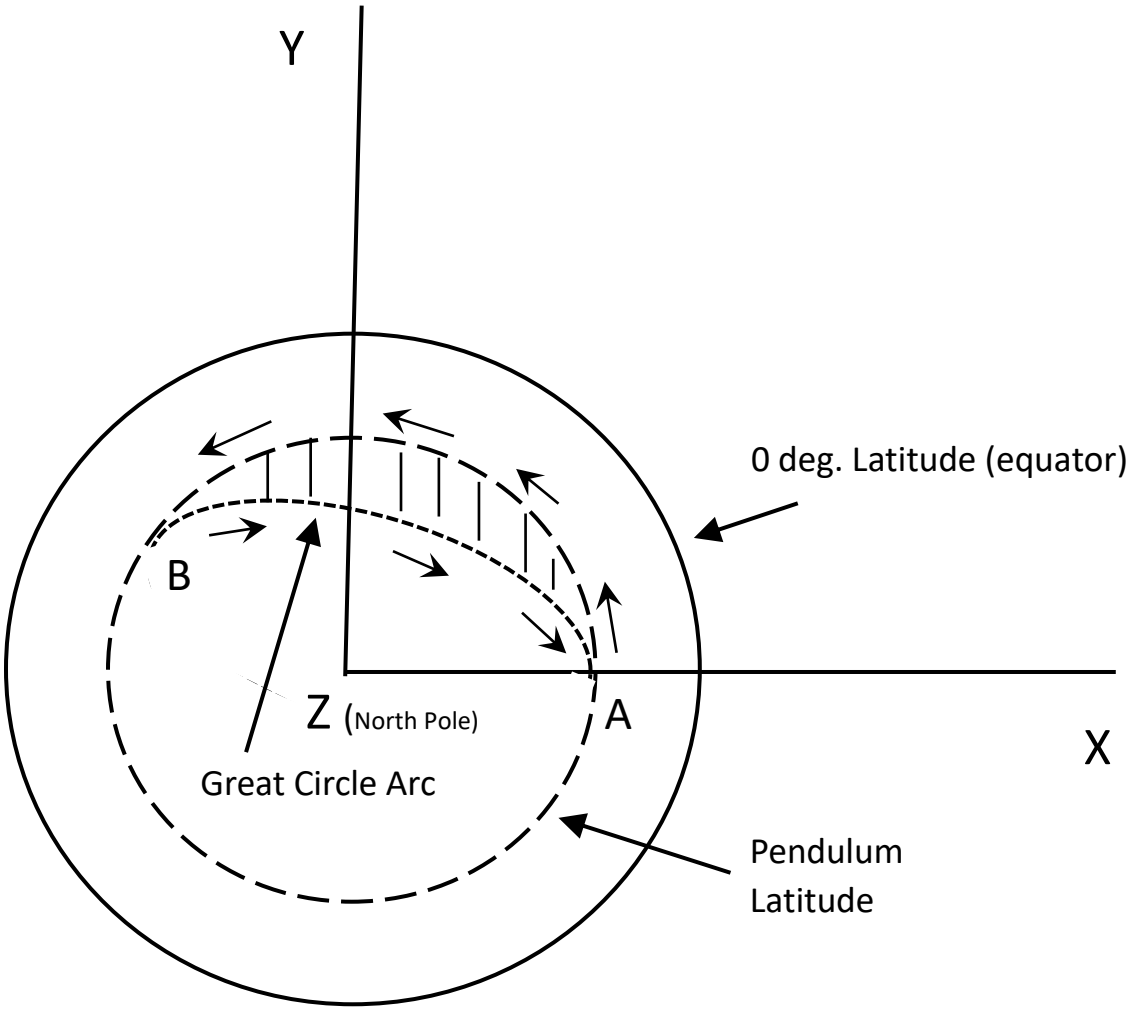

Fig. 3. The absolute rotation of the pendulum's vertical axis, as it moves from location **A** to **B** is defined by the solid angle region bounded by the arrows defining the constant latitude and Great Circle arcs.

Fig. 4 defines the relevant geometry that is used in eq. (9), where the true spherical geometry is represented on a flat plane for clarity. The unit vectors **a** and **b** are aligned with the axes **A** and **B**, respectively, and are defined in eq. (10), where Θ is the latitude and λ is the rotation of the Earth about its spin axis.

$$\mathbf{a} = \begin{pmatrix} \cos(\Theta) \\ 0 \\ \sin(\Theta) \end{pmatrix} \qquad \mathbf{b} = \begin{pmatrix} \cos(\Theta)\cos(\lambda) \\ \cos(\Theta)\sin(\lambda) \\ \sin(\Theta) \end{pmatrix} \tag{10}$$

The unit vector **e** is normal to axis **b** and is defined by eq. (11). The unit vector **f** is also normal to axis **b** and is defined in eq. (12).

$$\mathbf{e} = \mathbf{z} \times \mathbf{b} = \begin{bmatrix} -\sin(\lambda) \\ \cos(\lambda) \\ 0 \end{bmatrix} \tag{11}$$

$$\mathbf{f} = \mathbf{e} \times \mathbf{b} = \begin{bmatrix} \sin(\Theta)\cos(\lambda) \\ \sin(\Theta)\sin(\lambda) \\ -\cos(\Theta) \end{bmatrix} \tag{12}$$

The unit vector **d** is normal to the plane that defines the great circle arc connecting **a** and **b**, and is defined by eq. (13). The magnitude of **d** is given by eq. (14).

$$\mathbf{d} = \frac{\mathbf{a}\times\mathbf{b}}{|\mathbf{a}\times\mathbf{b}|} = \left[\frac{\cos(\Theta)}{|\mathbf{d}|}\right] \begin{bmatrix} -\sin(\Theta)\sin(\lambda) \\ \sin(\Theta)\cos(\lambda) - \sin(\Theta) \\ \cos(\Theta)\sin(\lambda) \end{bmatrix} \tag{13}$$

$$|\mathbf{d}| = \cos(\Theta)\sqrt{sin^2(\lambda) + sin^2(\Theta)[\cos(\lambda) - 1]^2} \tag{14}$$

The rotation of the axis as it moves around the solid angle region is the sum of the rotations at orientation **b** and at orientation **a** plus the continuous rotation as the axis slews from **a** to **b** along the constant latitude trajectory. The rotation of the axis at orientation **b** is given by the angle between **f** and **d**, which is given by eq. (15), where G is given by eq. (16).

$$\Gamma = cos^{-1}(\mathbf{f} \cdot \mathbf{d}) = cos^{-1}\left[\frac{-\sin(\lambda)}{G}\right] \tag{15}$$

$$G = \sqrt{sin^2(\lambda) + sin^2(\Theta)[\cos(\lambda) - 1]^2} \tag{16}$$

Due to symmetry, the rotation of the axis at orientation **a** is the same as the rotation at orientation **b**. The rotation due to the continuous rotation as the axis moves from orientation **a** to orientation **b** is given by λ sin(Θ). Therefore using eq. (9), the solid angle of the enclosed region is given by eq. (17).

$$\Omega = 2(\pi - \Gamma) - \lambda \sin(\Theta) \tag{17}$$

The analytical solution for the solid angle given by eq. (17) is also the rotation of the pendulum's vertical axis after the Earth rotates by angle λ.

The MF rotates according to eq. (17) but has the additional rotation caused by the Earth's angular rate of λ sin(Θ), as shown in eq. (18).

$$\psi = 2(\pi - \Gamma) - \lambda \sin(\Theta) + \lambda \sin(\Theta) = 2(\pi - \Gamma) \tag{18}$$

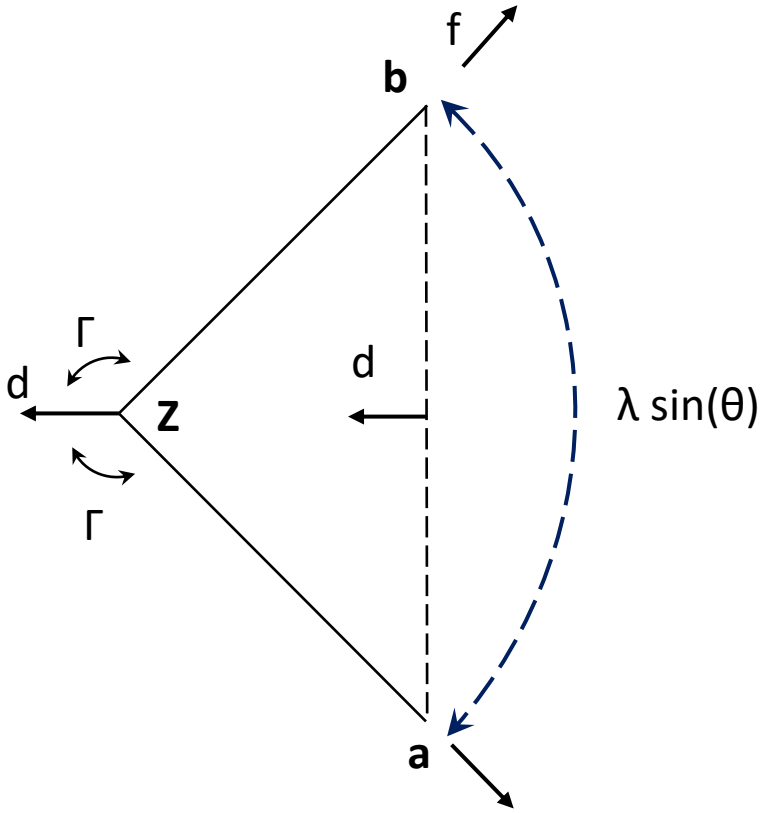

Fig. 4. Geometry related to eqs. (9 - 17) where the solid angle is bounded by the dashed lines.

For the special case λ = 2 π, Γ = 0 and the solid angle in eq. (17) is given by eq. (19), as expected for a complete rotation of the Earth on its axis. Eq. (20) contains the result for another special case, λ = π, Γ = π/2.

$$\Omega = 2\pi\,[1 - \sin(\Theta)] \quad (\lambda = 2\pi) \tag{19}$$

$$\Omega = \pi\,[1 - \sin(\Theta)] \quad (\lambda = \pi) \tag{20}$$

The MF rotates according to eq. (18) and has rotation angles corresponding to values of λ of 2π and π, respectively, as given in eqs. (21) and (22).

$$\psi = 2\,\pi \qquad (\lambda = 2\pi) \tag{21}$$

$$\psi = \pi \qquad (\lambda = \pi) \tag{22}$$

The rotation of the pendulum's vertical axis and that of its MF for values other than the special cases of λ = 2 π and λ = π must be evaluated using eqs. (15 – 18). For values of λ greater than 2π, one can sum the rotations for each complete Earth rotation given by eq. (19) and add the residual rotation value obtained from eq. (17) using λ mod 2π, which accounts for the remaining partial rotation. A similar method can be used for the MF using eqs. (18) & (21).

The analytical solution for the rotation angle of the pendulum given by eq. (17) permits the derivation of the rate of change of Ω by simple differentiation, as shown in eq. (23), with dΓ/dt given in eq. (24).

$$\frac{d\Omega}{dt} = -2\frac{d\Gamma}{dt} - \sin(\Theta)\frac{d\lambda}{dt} = -2\sin(\Theta)\,[\cos(\lambda) - 1]\,G^{-2}\frac{d\lambda}{dt} - \sin\,(\Theta)\frac{d\lambda}{dt} \tag{23}$$

$$\frac{d\Gamma}{dt} = \frac{-sin^2(\Theta)}{\sin\,(\Gamma)}\,[1 - \cos(\lambda)]^2\;G^{-3}\;\frac{d\lambda}{dt} = \;\sin(\Theta)\,[\cos(\lambda) - 1]\;G^{-2}\;\frac{d\lambda}{dt} \tag{24}$$

Since the MF has an additional rotation rate of sin(Θ) dλ /dt due to the rotation of the Earth, its rotation rate, dψ/dt is given by eq. (25).

$$\frac{d\psi}{dt} = -2\frac{d\Gamma}{dt} = -2\sin(\Theta)\,[\cos(\lambda) - 1]\;G^{-2}\;\frac{d\lambda}{dt} \tag{25}$$

The angular rate of the pendulum rotation given by eq. (23) can be used to obtain the ratio of the pendulum rotation rate and the Earth rotation rate, as given by eq. (26). Likewise using eq. (25), the ratio of the MF rotation rate and the Earth rotation rate is given by eq. (27).

$$\frac{d\Omega}{d\lambda} = -2\sin(\Theta)\,[\cos(\lambda) - 1]G^{-2} - \sin\,(\Theta) \tag{26}$$

$$\frac{d\psi}{d\lambda} = -2\sin(\Theta)\,[\cos(\lambda) - 1]\;G^{-2} \tag{27}$$

3. Absolute Rotation for a Moving Pendulum

An absolute rotation about the pendulum's vertical axis can be generated, if the axis slews in an inertial reference frame. The slewing motion for a pendulum fixed on the surface of the Earth is created by the Earth's spin rate. If the Earth's spin rate is zero, and the pendulum moves along the surface of the Earth, a slewing motion of the pendulum axis is created and can produce an absolute rotation of the pendulum's vertical axis. Let a pendulum's vertical axis be defined by the vector **R**, which extends from the center of the Earth to the Earth's surface, as shown in Fig. 5. The motion of the pendulum on the Earth's surface is driven by a rotation of σ about axis **P** over a time, T, which moves the pendulum from point **A** to point **B.** The Earth rotates simultaneously about the z-axis by angle λ over a time T, which moves the pendulum from point **B** to point **C**. Since the rotations occur simultaneously, the actual trajectory of the pendulum is the solid line that connects point **A** directly to point **C**, as shown in Fig. 5. The movement of the pendulum is due to its total attitude transformation, **U**, which can be obtained using

a sequence of incremental rotations about the Earth's spin axis or z-axis and the axis **P**. The angular rates about the **P** and **z** axes are given by the magnitudes of $\boldsymbol{\omega}_P$ and $\boldsymbol{\omega}_Z$, respectively, as shown in eq. (28).

$$\omega_P = |\boldsymbol{\omega}_P| = \frac{\sigma}{T}, \qquad \omega_Z = [\boldsymbol{\omega}_Z] = \frac{\lambda}{T} \tag{28}$$

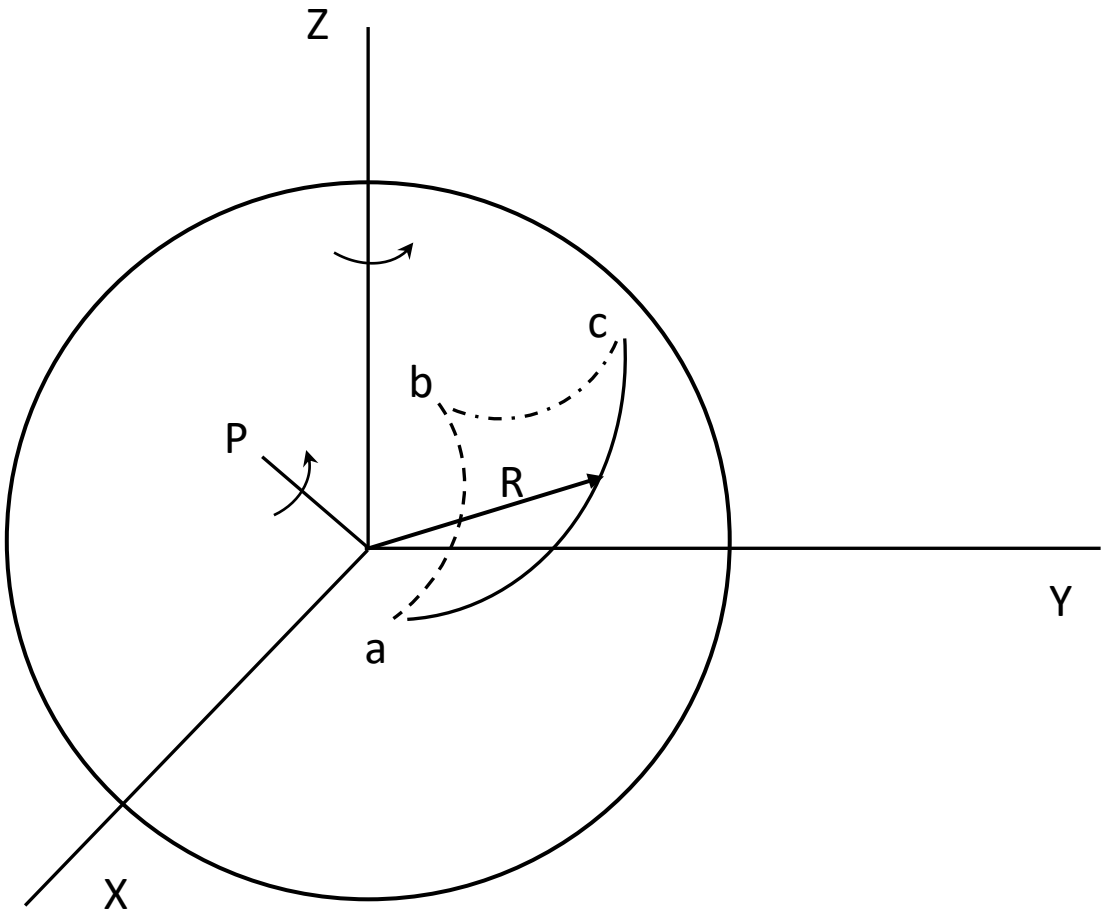

Fig. 5. Slewing motion of a pendulum going from **A** to **C** , as it is driven by a rotation about axis **P** and the spinning motion of the Earth about the **z**-axis.

The first step in obtaining **U** is to update **P** and **R** using an incremental rotation about the z-axis using the transformation matrix $\mathbf{U}_{Zi}$ defined in eq. (29), where Δt is the associated time increment.

$$\mathbf{U}_{Zi} = \mathbf{U}(\mathbf{z}, \boldsymbol{\omega}_Z \Delta t) \tag{29}$$

Once **P** is update by $\mathbf{U}_{Zi}$, it is used to move **R** across the surface of the Earth via the transformation matrix $\mathbf{U}_{Pi}$, given in eq. (30). The updated equations for **P** and **R** are given by eqs. (31) & (32), respectively.

$$\mathbf{U}_{Pi} = \mathbf{U}(\mathbf{P}_{i+1}, \boldsymbol{\omega}_P \Delta t) \tag{30}$$

$$\mathbf{P_{i+1}} = \mathbf{U_{Zi}}\,\mathbf{P_i} \tag{31}$$

$$\mathbf{R_{i+1}} = \mathbf{U_{Pi}}\,\mathbf{U_{Zi}}\,\mathbf{R_i} \tag{32}$$

Eqs. (29-32) are used repeatedly to update both **P** and **R**. The total transformation matrix, $\mathbf{U_n}$, used to propagate **R** from **A** to **C** is given by eq. (33), where $\mathbf{V_i}$ is given in eq. (34).

$$\mathbf{U_n} = \mathbf{V_n}\,\mathbf{V_{n-1}}\,\mathbf{V_{n-2}}\,\mathbf{V_{n-3}} \ldots\ldots \mathbf{V_1} \tag{33}$$

$$\mathbf{V_i} = \mathbf{U_{Pi}}\,\mathbf{U_{Zi}} \tag{34}$$

The locations of **R** and **P** at the i^{th} time step are given by eqs. (35) and (36), where **R** is transformed by the incremental rotations about **P** and **z**, as given by eq. (33), and **P** is transformed only by the rotation about **z,** as given by eq. (36). Since the z-axis remains fixed in the Earth's frame the time increment Δt in eq. (29) can be replaced by the total time to the i^{th} time step in eq. (36).

$$\mathbf{R_i} = \mathbf{U_i}\,\mathbf{R_1} \tag{35}$$

$$\mathbf{P_i} = \mathbf{U}(\mathbf{z}, \boldsymbol{\omega}_\mathbf{z}\, t_i)\,\mathbf{P_1} \tag{36}$$

The rotational transformation about **R** is computed by first evaluating the rotational increments at the i^{th} time step and then summing them to obtain the total rotation about **R**. The component of each angular increment along **R** is computed at each time step via the dot product between **R** and the **z**-axis, as well as, the dot product between **R** and **P**, as given in eq. (37).

$$S_i = \frac{(\mathbf{R_i}\cdot\mathbf{z})\,\omega_Z\,\Delta t}{|\mathbf{R_i}|} + \frac{(\mathbf{R_i}\cdot\mathbf{P_i})\,\omega_P\,\Delta t}{|\mathbf{R_i}||\mathbf{P_i}|} \tag{37}$$

The total rotation about **R** is the integral of the angular rate along **R** and is found by summing S_i , as shown in eq. (38), where $\mathbf{S_1} = 0$ at t = 0. A more accurate numerical integration scheme can be used to replace eqs. (37) and (38), if needed.

$$S = \sum_1^N S_i \tag{38}$$

The total attitude transformation given by eq. (33) can be used to transform $\mathbf{R_1}$ to $\mathbf{R_N}$, as given in eq. (39).

$$\mathbf{R_N} = \mathbf{U}\,\mathbf{R_1} \tag{39}$$

The total rotation about **R** includes the integral of the angular rate given by S and the solid angle bounded by the actual trajectory of **R** and the return trajectory of **R** along a great circle arc. The return attitude transformation, $\mathbf{U_G}$, along the great circle arc trajectory can be computed easily using the Pivot Parameter methodology (Patera, 2017) and is given by eq. (40), where **C** is the unitized average of $\mathbf{R_1}$ and $\mathbf{R_N}$, as shown in eq. (41).

$$\mathbf{U_G} = \mathbf{U}(\mathbf{C}, 180)\,\mathbf{U}(\mathbf{R_1}, 180) = \mathbf{U}(\mathbf{R_N}, 180)\,\mathbf{U}(\mathbf{C}, 180) \tag{40}$$

$$\mathbf{C} = \frac{\frac{(\mathbf{R_1}+\mathbf{R_N})}{2}}{\left|\frac{(\mathbf{R_1}+\mathbf{R_N})}{2}\right|} = \frac{\mathbf{R_1}+\mathbf{R_N}}{|\mathbf{R_1}+\mathbf{R_N}|} \tag{41}$$

The total transformation, $\mathbf{U_T}$, includes the actual trajectory and the return great circle arc trajectory as given by eq. (42).

$$\mathbf{U_T = U\,U_G} \tag{42}$$

The magnitude of the associated Euler Rotation Vector, ψ, is the solid angle of the region bounded by the closed loop trajectory of **R** plus the integral of the angular rate along **R** and is also equal to the rotation of the MF about its vertical axis. Since the pendulum absolute rotation, Ω, does not include the integral of the angular rate along its vertical axis, it has a rotation angle equal to that of the MF minus S, as shown in eq. (43).

$$\Omega = \psi - S \tag{43}$$

Therefore, the pendulum has a rotation about its vertical axis of Ω and the MF has a rotation about its vertical axis of ψ.

These results are for the motion caused by a single auxiliary axis driving the motion of the pendulum. One can use several auxiliary axes with different orientations in sequence to drive the motion of the pendulum along the surface of the Earth. The associated absolute rotations can be combined to obtain the total absolute rotation. A sufficiently large number of auxiliary axes can generate any translational motion of the pendulum that is desired, as well as, its absolute rotation.

4. Numerical Results

The rotation of the Foucault Pendulum was computed using eq. (17) for various values of latitude, θ, and Earth rotation angle, λ, as shown in Table 1. Results were validated using the general method of solid angle calculation (Patera, 2020b) involving eq. (7) to ensure that the analytical solution was correct. For each latitude value, the rotation angle of the pendulum is not a linear function of Earth rotation angle, although the values at 180 degrees of Earth rotation are one half the values at 360 degrees.

The behavior of the pendulum rotation angle is displayed in Figs. 6, 8, 10, 12 & 14, which also include the rotation of the MF. Notice that for a complete rotation of the Earth, the rotation angle of the MF is 360 degrees for each value of latitude. The solid angle contribution to the MF's rotation angle becomes smaller and the Earth rotation rate contribution becomes larger for larger values of latitude. For 180 degrees of Earth rotation the MF rotates 180 degrees for each latitude. Each pendulum rotation angle at 180 degrees of Earth rotation is one half its value at 360 degrees of Earth rotation. This is due to symmetry of the solid angle of the spherical cap, i.e., solid angle equals π [1-sin(Θ)] for each 180 degrees of Earth rotation. The rotation angle rate in terms of the Earth rotation rate for the pendulum and MF are presented in Figs. 7, 9, 11, 13 & 15. The highest rates occur near the Earth rotation angle of 180 degrees. The nonlinear dependence of pendulum rotation angle and associated rate on the Earth rotation angle becomes larger for smaller values of latitude as shown in Figs. 12, 13, 14 & 15. For extremely small values of latitude, the pendulum has rotation angles that approach 360 degrees because that is the solid angle of the Northern Hemisphere, as shown in Figs. 14 & 15. Although the pendulum's precession rate decreases as latitude becomes small, its absolute rotation angle becomes larger and approaches 360 degrees. In all cases, the difference between the pendulum rate and the MF rate agrees with the known pendulum precession rate of -ω sin(Θ) for all values of Earth rotation angle.

Table 1
Absolute Rotation Angle Examples for Algorithm Validation

Earth rotation angle, deg.	Pendulum angle, deg. 30 deg. Lat.	Pendulum angle, deg. 45 deg. Lat.	Pendulum angle, deg. 60 deg. Lat.
45	0.902	0.83	0.4967
90	8.13	6.89	3.84
135	33.22	23.82	11.96
180	90	52.72	24.12
225	146.78	81.62	36.27
270	171.87	98.55	44.39
315	179.10	104.61	47.73
345	179.97	105.41	48.21
360	180	105.44	48.23

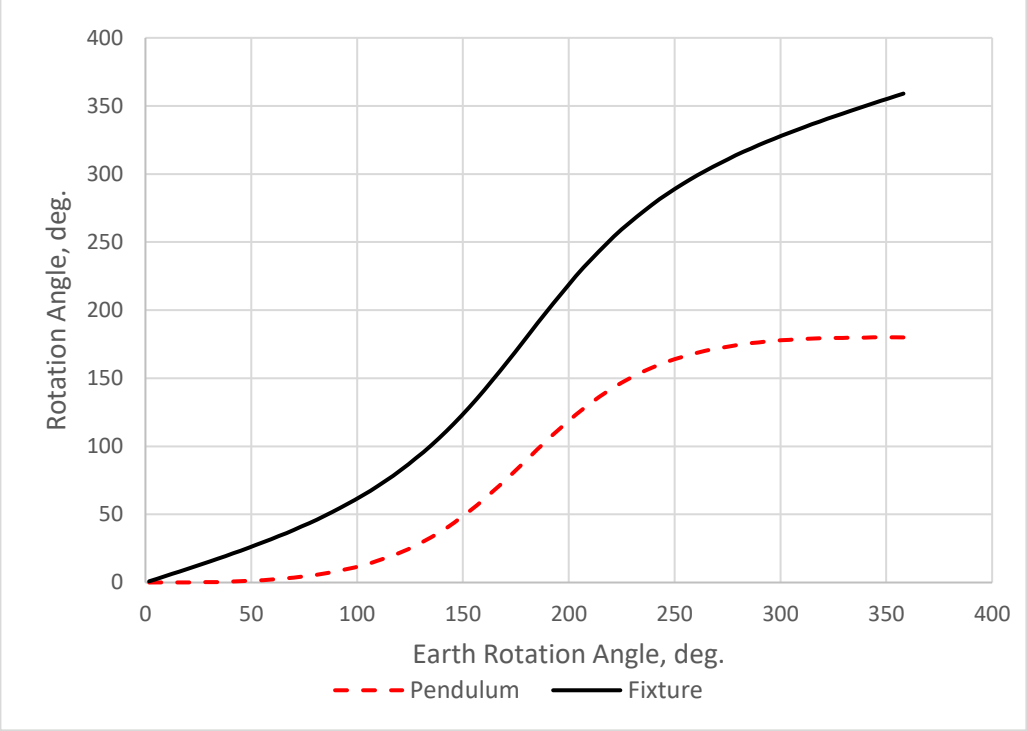

Fig. 6. Pendulum and fixture rotation angles versus the Earth rotation angle for 30 deg. latitude.

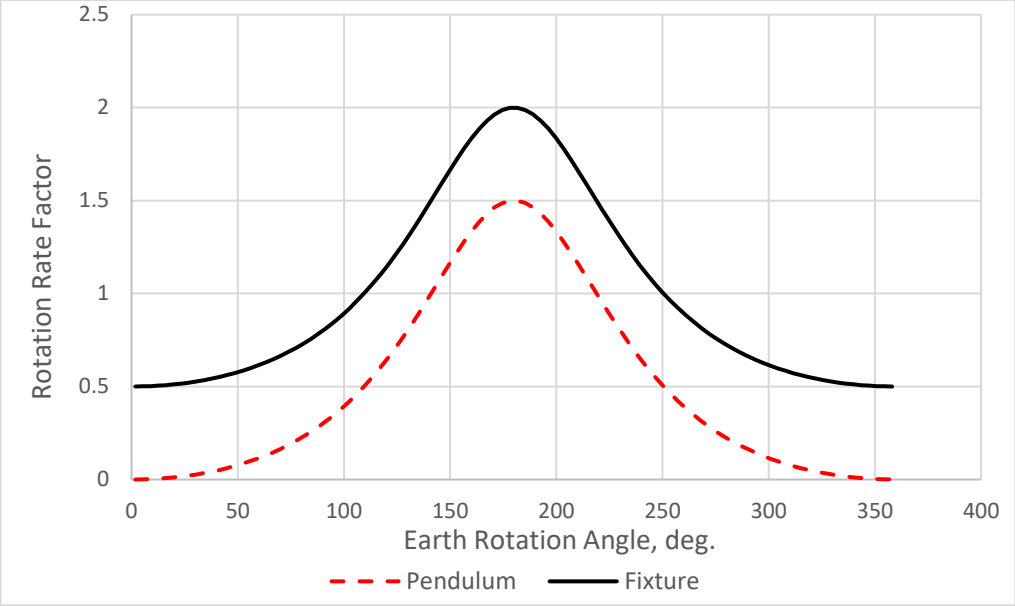

Fig. 7. Rotation rates in terms of the Earth rotation rate for 30 deg. latitude.

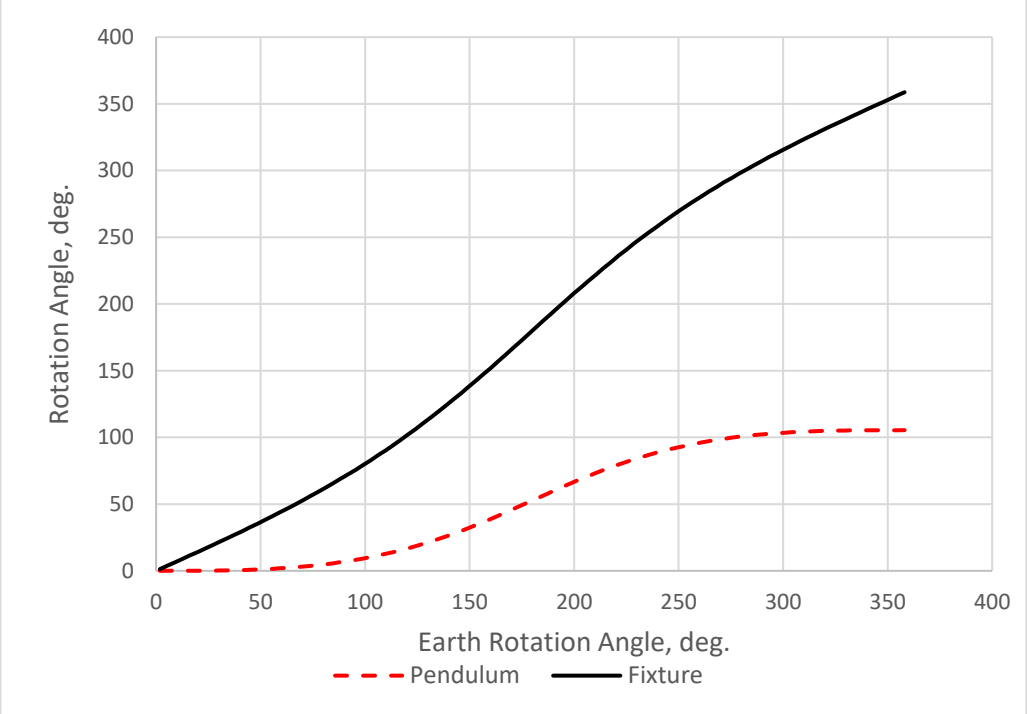

Fig. 8. Pendulum and fixture rotation angles versus the Earth rotation angle for 45 deg. latitude.

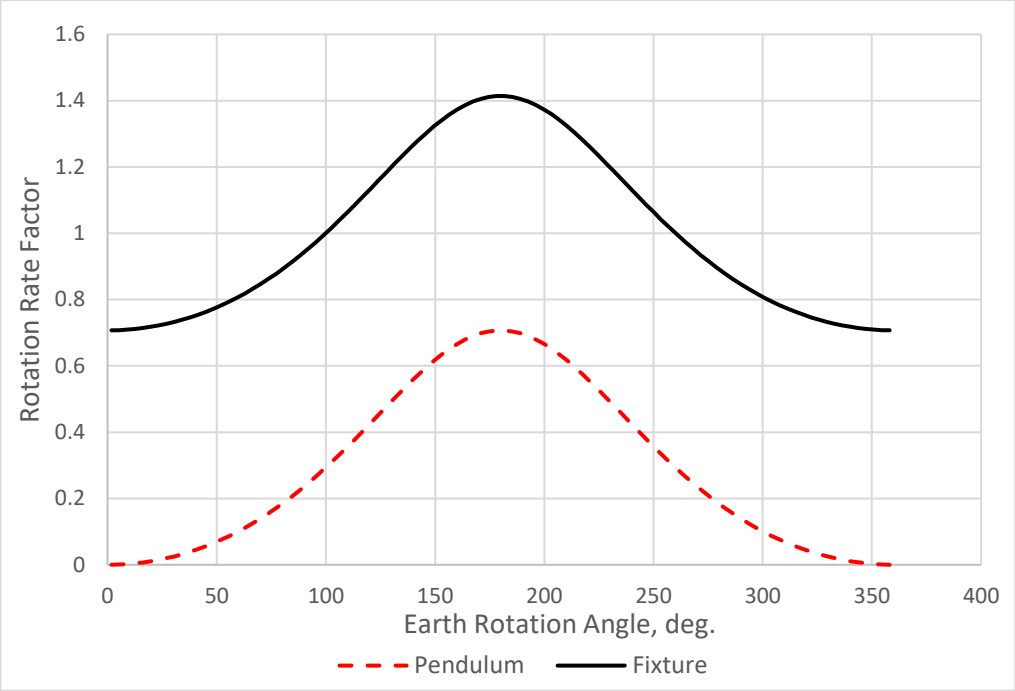

Fig. 9. Rotation rates in terms of the Earth rotation rate for 45 deg. latitude.

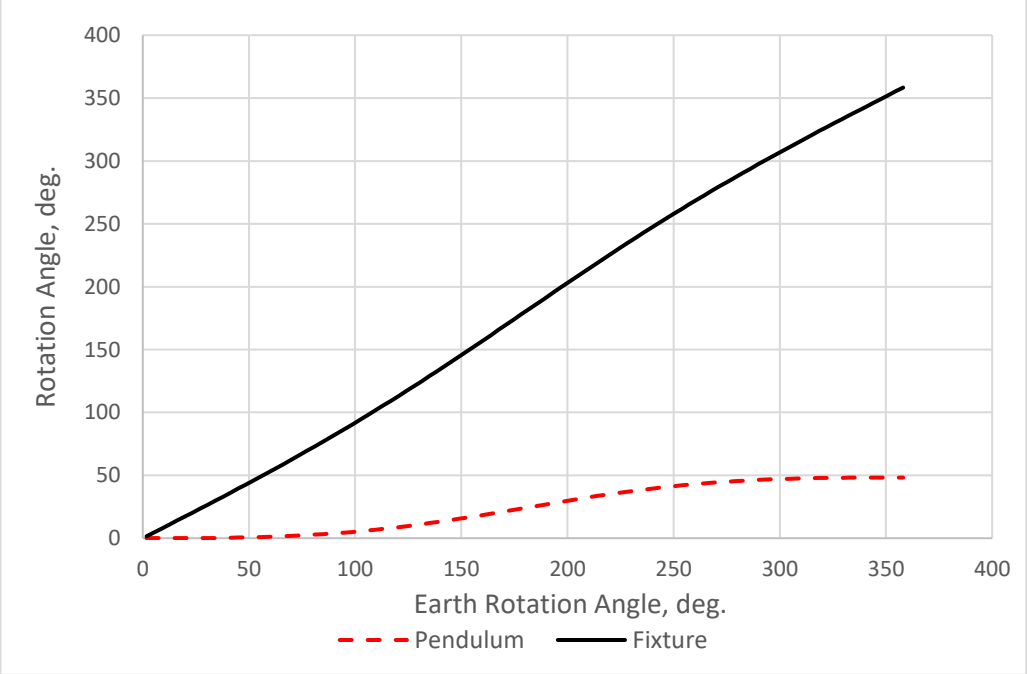

Fig. 10. Pendulum and fixture rotation angles versus the Earth rotation angle for 60 deg. latitude.

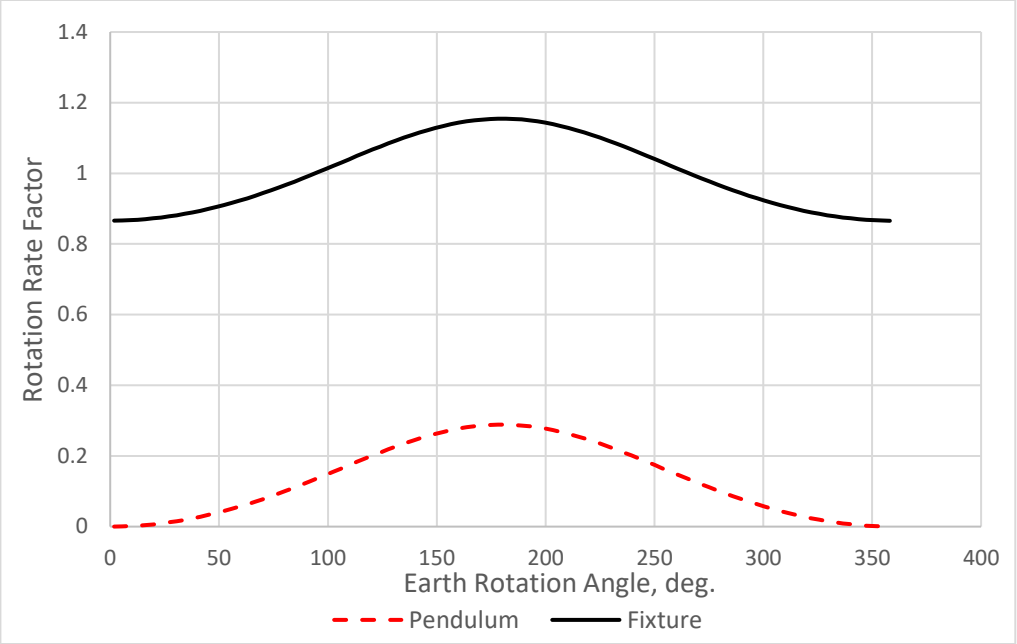

Fig. 11. Rotation rates in terms of the Earth rotation rate for 60 deg. latitude.

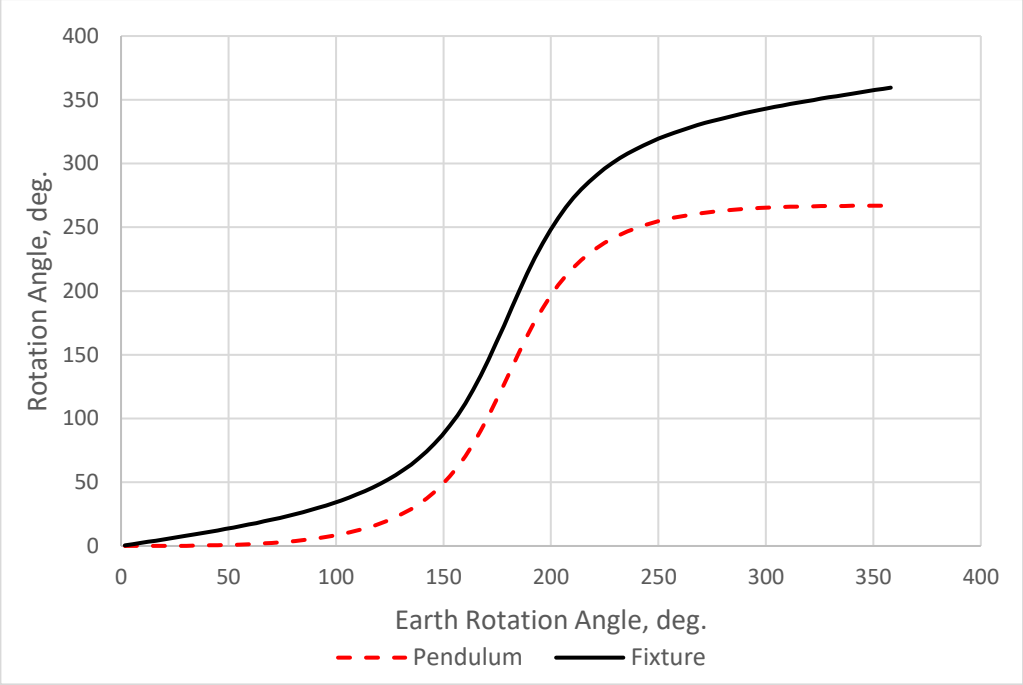

Fig. 12. Pendulum and fixture rotation angles versus the Earth rotation angle for 15 deg. latitude.

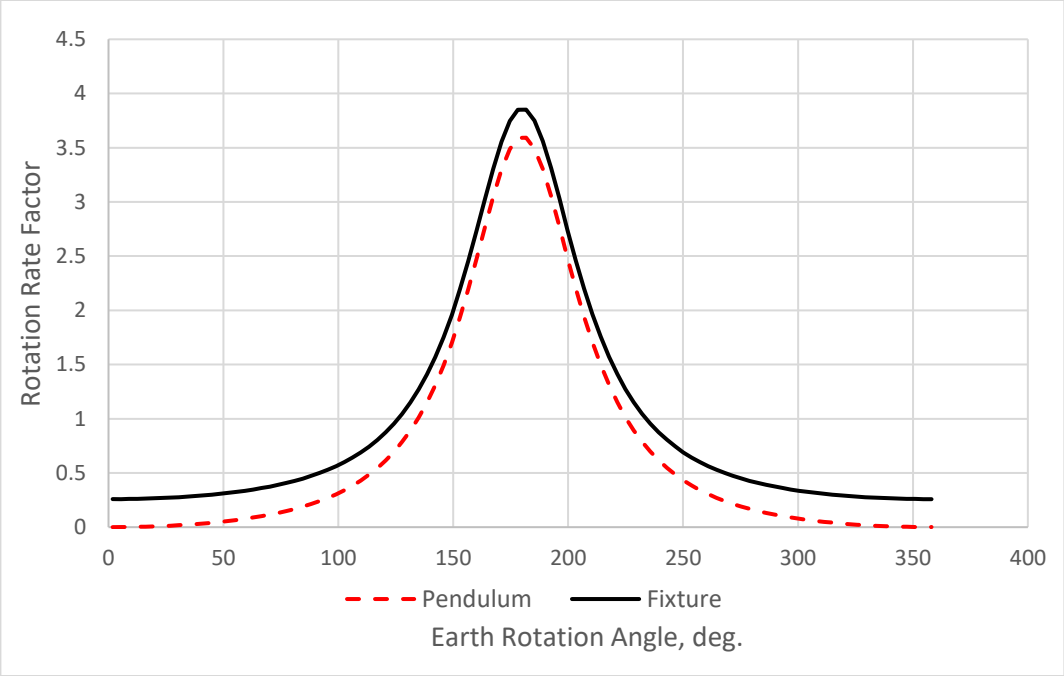

Fig. 13. Rotation rates in terms of the Earth rotation rate for 15 deg. latitude.

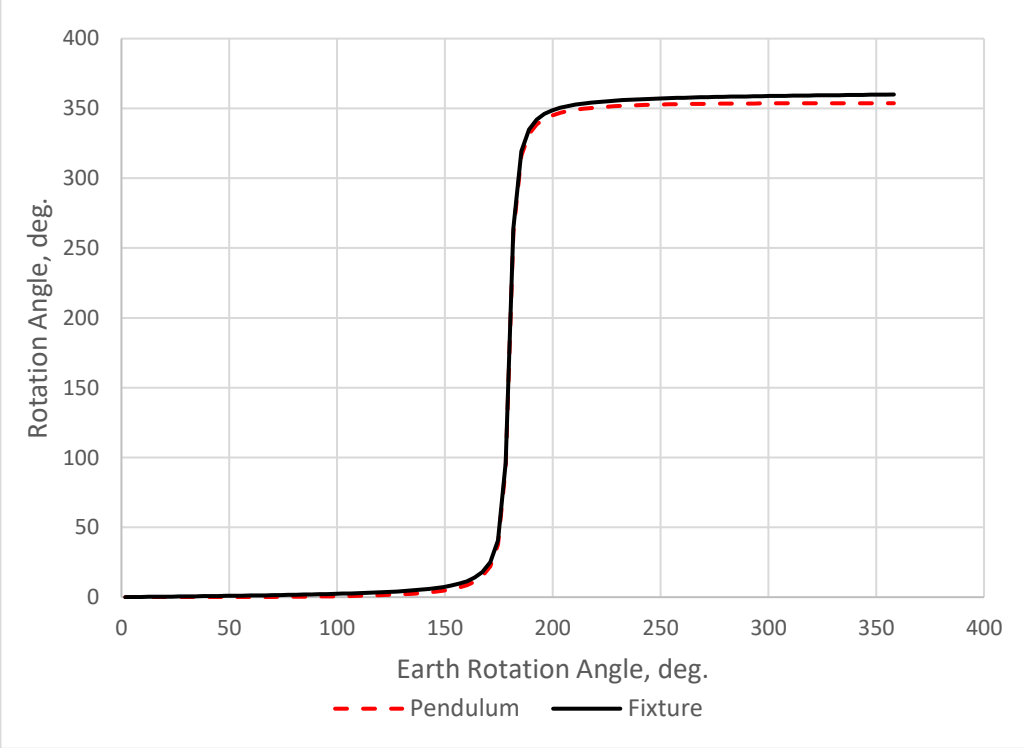

Fig. 14. Pendulum and fixture rotation angles versus the Earth rotation angle for 1 deg. latitude.

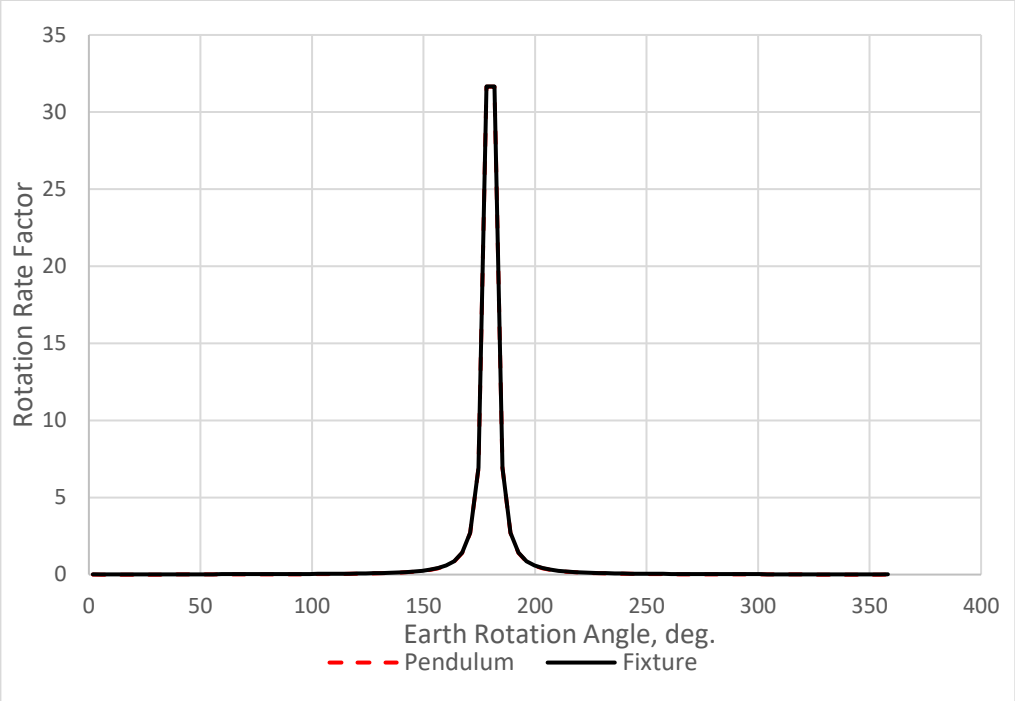

Fig. 15. Rotation rates in terms of the Earth rotation rate for 1 deg. latitude.

5. Numerical Results for a Traveling Pendulum

A simulation was developed using the method presented in Section 3 to compute the absolute rotation for a traveling pendulum. The pendulum is assumed to travel smoothly along the surface of the Earth, which is assumed spherical, and not be subject to vibrations and external forces, etc. that would disturb its motion. The pendulum is initially located in Los Angeles (34.0522 N, -118.2437 W) and travels to Quebec City, Canada (46.8131 N, -71.2075 W) along a great circle arc. The arc is generated by a rotation of 37.37 deg. about the axis (-0.2791, 0.6744, 0.6836), as shown in Fig.16. No consideration is given to the mode of travel, although one can envision a high speed magnetically levitated train to make the abstraction more concrete. The pendulum moves at a constant rate and reaches Quebec City in 24 hours or one complete rotation of the Earth. The absolute rotation of the vertical axes of both the traveling pendulum and its MF are shown in Fig. 17. The absolute rotations of the stationary pendulum and its MF are also shown in Fig. 17 for comparison purposes.

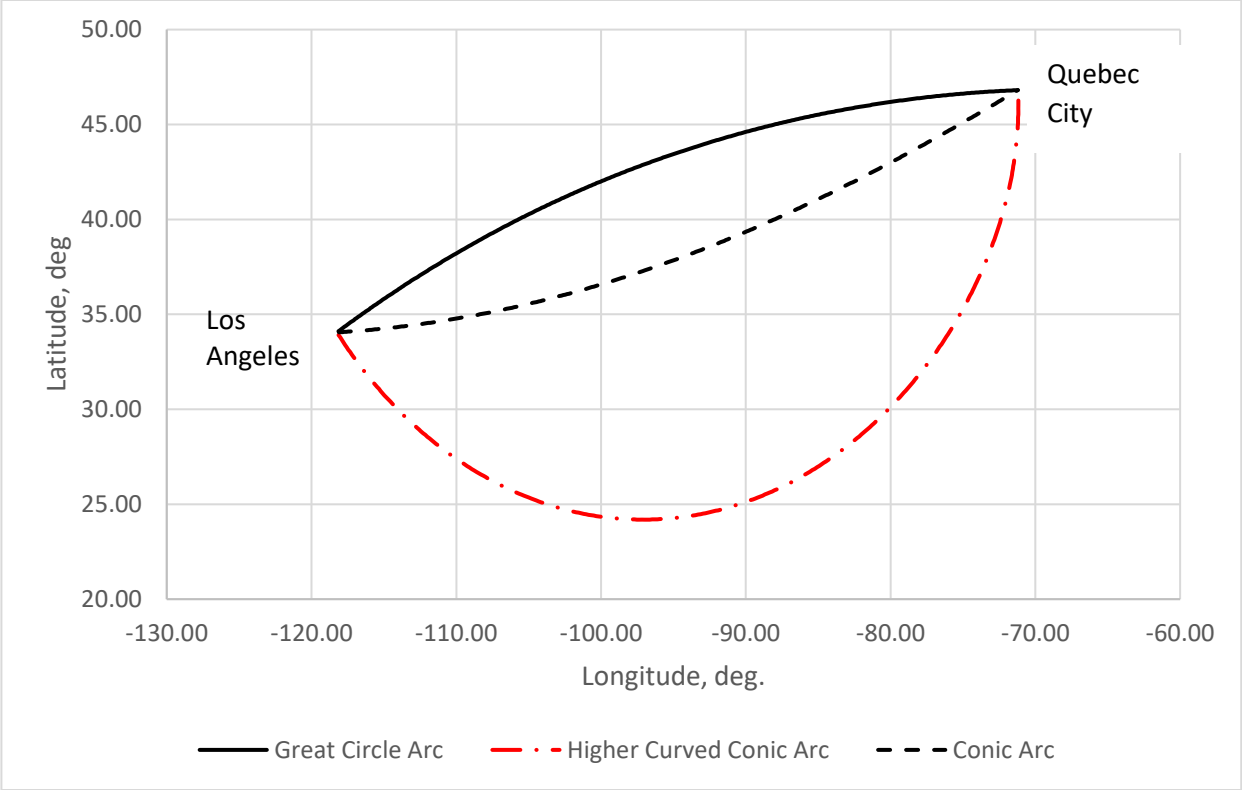

Fig. 16. Three different trajectories taken by the pendulum in moving from Los Angeles to Quebec City in terms of latitude and longitude.

The time derivative of each absolute rotation angle in Fig. 17 was computed numerically by the simulation and shown in Fig. 18. Note that the rotation rates illustrated in Fig. 18 are not purely angular rates, since the rotation rates include the rate of change of the associated solid angle, as well as the associated angular rate. The rotation rates in Fig. 18 are provided in terms of the Earth's angular rate, which clarifies the differences in the rates for the traveling pendulum when compared to the stationary pendulum.

The trajectory of the pendulum was altered by using a rotation of 71.85 degrees about the axis (-0.2104, -0.3283, 0.9208) to drive the pendulum from Los Angeles to Quebec City along a conical arc, as shown in Fig. 16. An additional pendulum trajectory was achieved with a 180 degree rotation about the axis (-0.0906, -0.7272, 0.6804), which results in a highly curved conical arc. A comparison of all three trajectories is presented in Fig. 16, which illustrates the pendulum trajectories in terms of latitude and longitude. Fig. 19 illustrates the comparison between the absolute rotations associated with the traveling and stationary pendulums. Fig. 20 shows the rate of change of the absolute rotations given in Fig. 19. As expected, the absolute rotations of the pendulum and its MF differ significantly from those in Figs. 17 and Fig. 18. Fig. 21 illustrates the comparison between the absolute rotations of the stationary pendulum and the traveling pendulum over the highly curved conical arc defined above. Fig. 22 shows the rate of change of the absolute rotations given in Fig. 21.

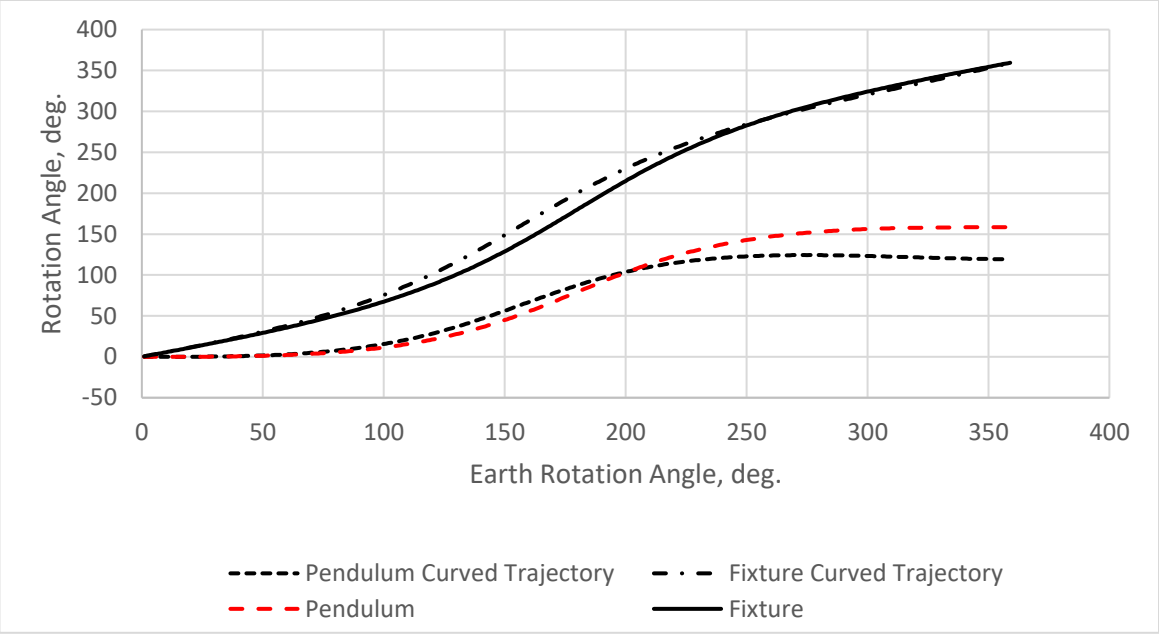

Fig. 17. Absolute rotations for pendulum fixed at latitude 34 deg. and a pendulum that travels from Los Angeles to Quebec City, Canada along a great circle arc of length 37.37 deg.

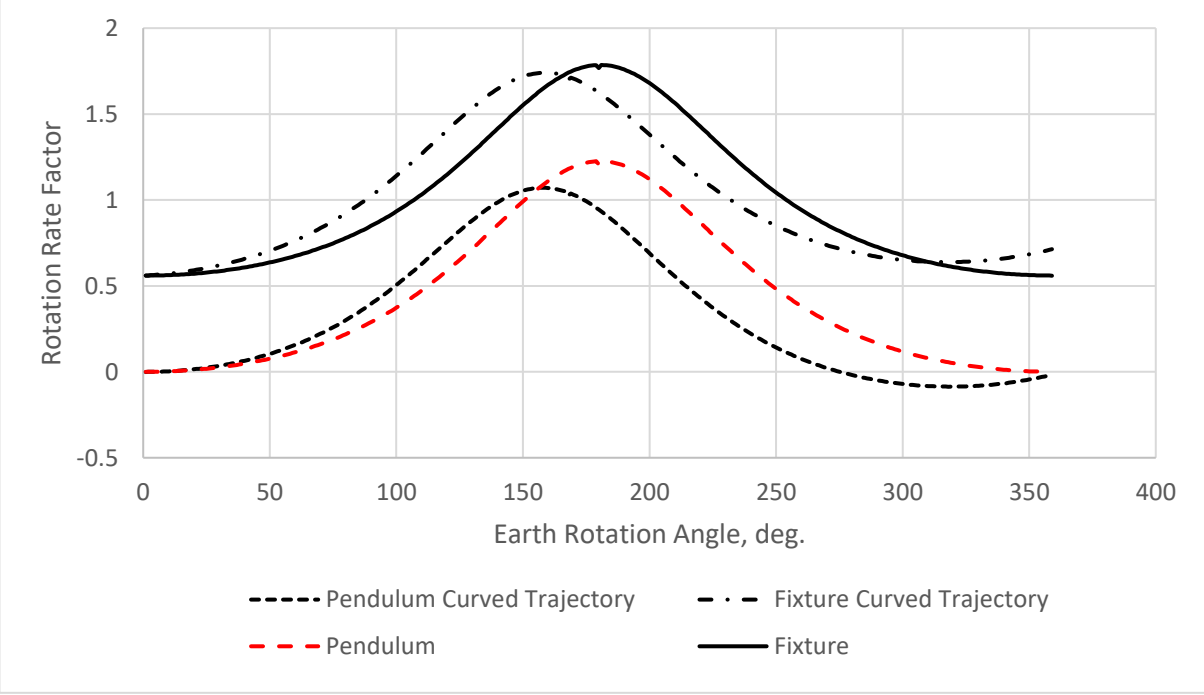

Fig. 18. The rotation rate factor comparisons for the stationary pendulum and the traveling pendulum referenced in Fig. 17.

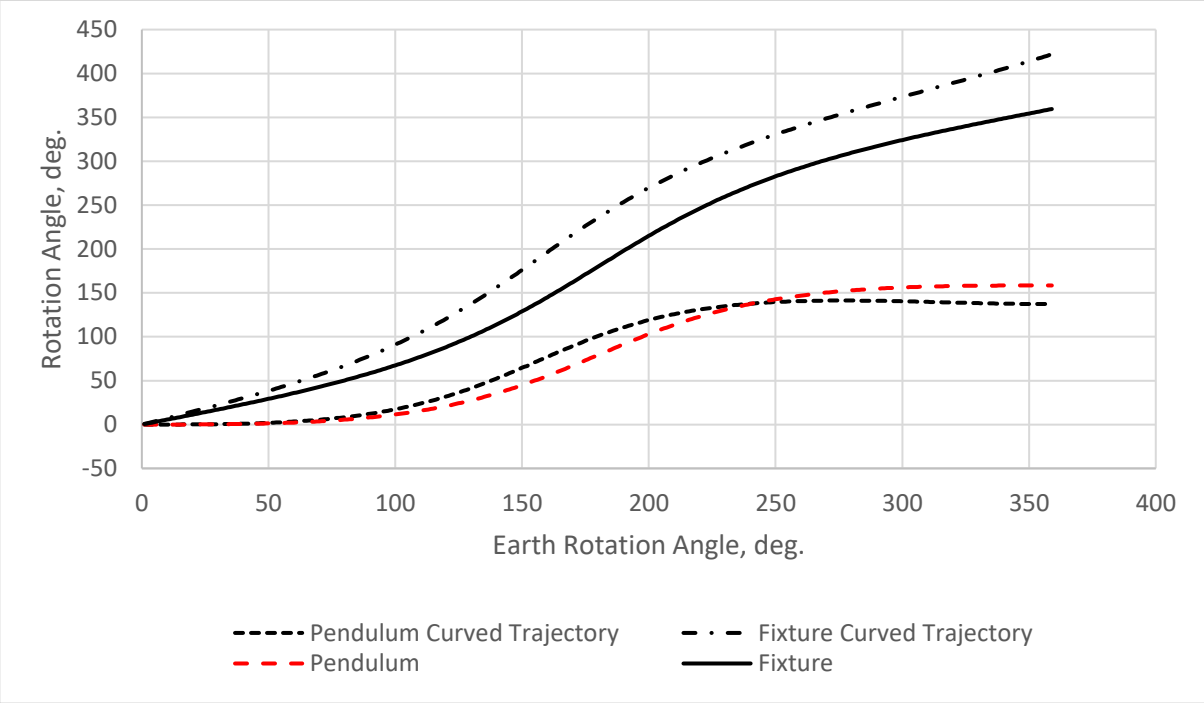

Fig. 19. Comparison of absolute rotations for a stationary pendulum and a traveling pendulum along a conical trajectory for a driving rotation angle of 71.85 deg. rather than a great circle arc shown in Fig. 17.

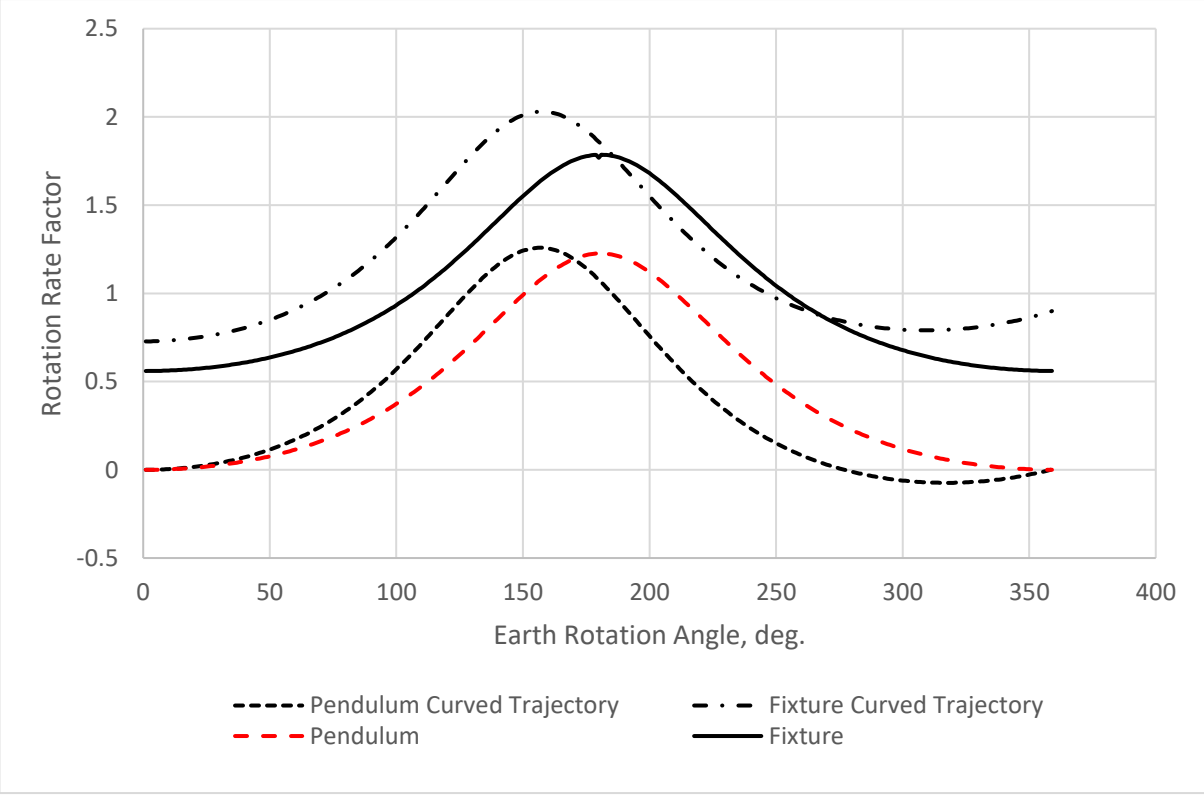

Fig. 20. Rotation rate factors for the example shown in Fig. 19.

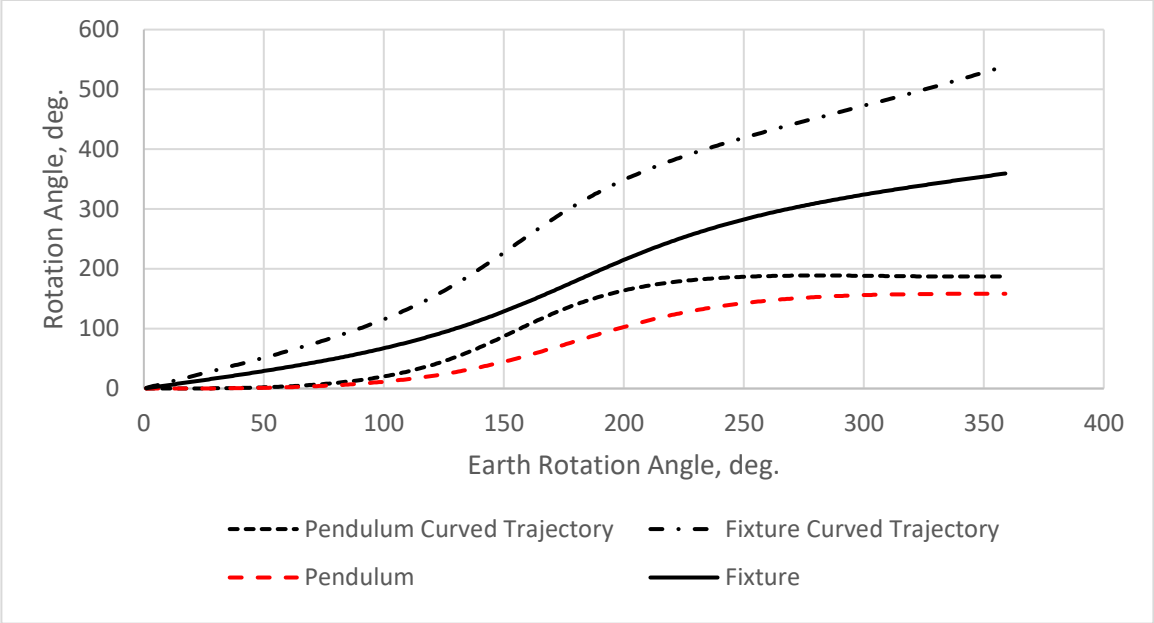

Fig. 21. Comparison of absolute rotations for a stationary pendulum and a traveling pendulum along a highly curved conical arc for a driving rotation angle of 180 deg. rather than a great circle arc shown in Fig. 17.

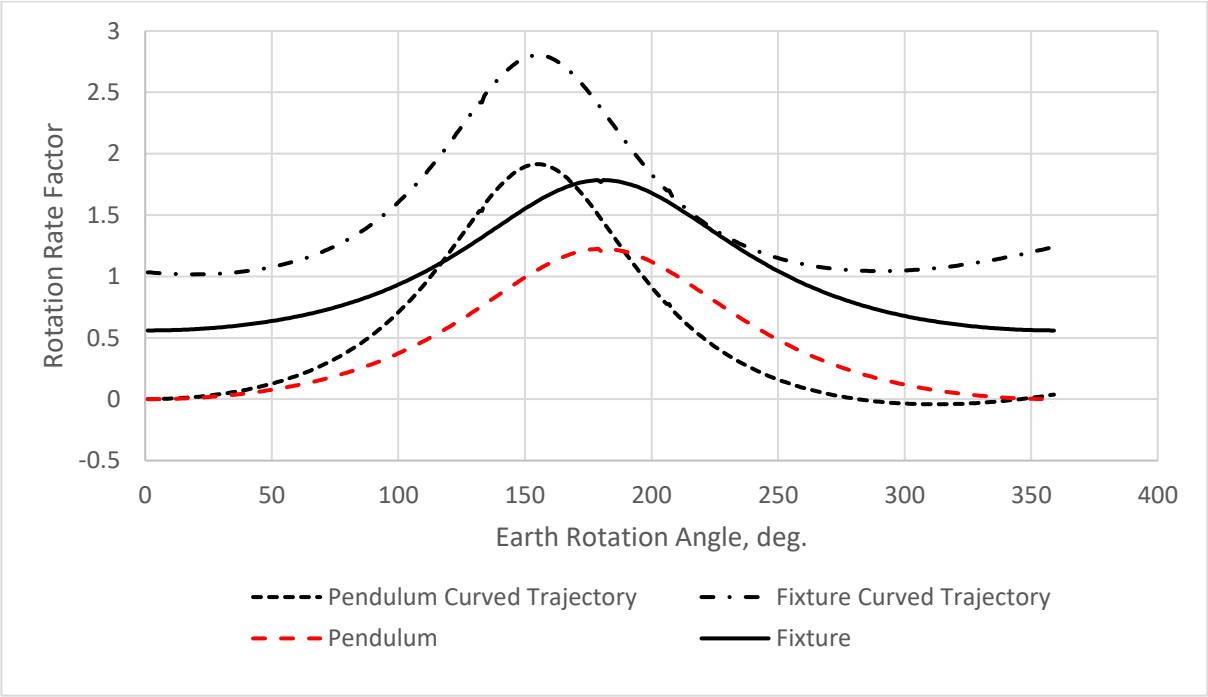

Fig. 22. Rotation rate factors for the example shown in Fig. 21.

The precession rates in terms of Earth angular rate for the cases in Figs. (17 - 22) are shown in Fig. 23. The horizontal constant precession rate represents a stationary pendulum. The great circle arc trajectory and the conical arc trajectories indicate variable precession frequencies that are greater than the stationary pendulum. The motion of the pendulum across the Earth's surface adds to its absolute rotation and associated precession frequency. For the case of a non-rotating Earth, the great circle arc trajectory between Los Angles and Quebec City does not impart absolute rotations to the pendulum and MF, as shown in Table 2. However, the conical trajectory and the highly curved conical trajectory do result in rotations of the MF and pendulum, as given in Table 2, which includes the rotation about each axis that drives the associated traveling motion.

Table 2
Absolute Rotations with a Non-rotating Earth

Case #	Pendulum Rotation, deg	Mounting Fixture Rotation, deg	Driving Motion Angle, deg
1. Great Circle Arc	0	0	37.37
2. Conic Arc	2.32	62.52	71.85
3. Highly Curved Arc	9.49	180.0	180.0

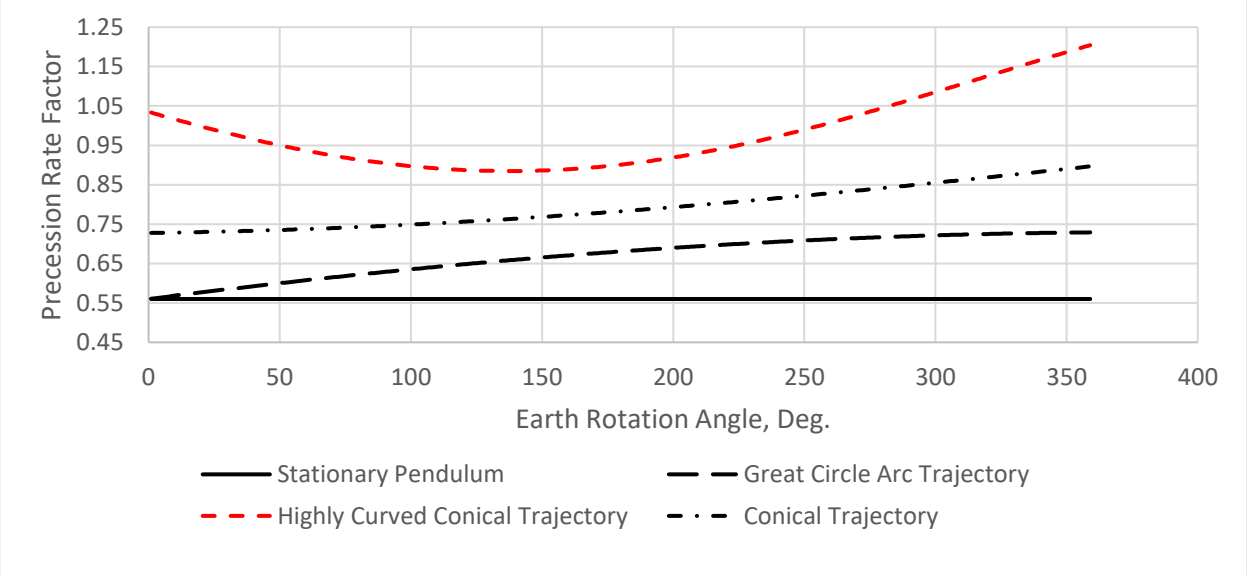

Fig. 23. Precession rate factors for the cases represented in Figs. (17 - 22) show that traveling pendulums have variable precession rates.

In the last example, the pendulum is located at (56.9478 N, -118.2437 W) on a non-rotating Earth but the pendulum travels, as it is driven by a rotation of 360 degrees about a vertical axis located at (0 N, -118.2437 W). Even though the Earth is not rotating, an absolute rotation about the pendulum's vertical axis is generated by its traveling motion over the curved Earth surface. The absolute rotations of this traveling pendulum and MF are compared to those of a similar pendulum located at Los Angeles (34.0522 N, -118.2437 W) on a spinning Earth, as shown in Fig. 24. The horizontal axis in Fig. 24 represents the rotation angle about the axis that drives the pendulum in each case. The absolute rotations are the same because the angular difference between the vertical

axis in Los Angeles and the Earth's spin axis is 56.9478 degrees, which is the same as the difference between the vertical axis of the traveling pendulum and the axis that drives its motion. The rate of change of the absolute rotation angles in Fig. 24 are provided in Fig. 25 and are also the same for both cases.

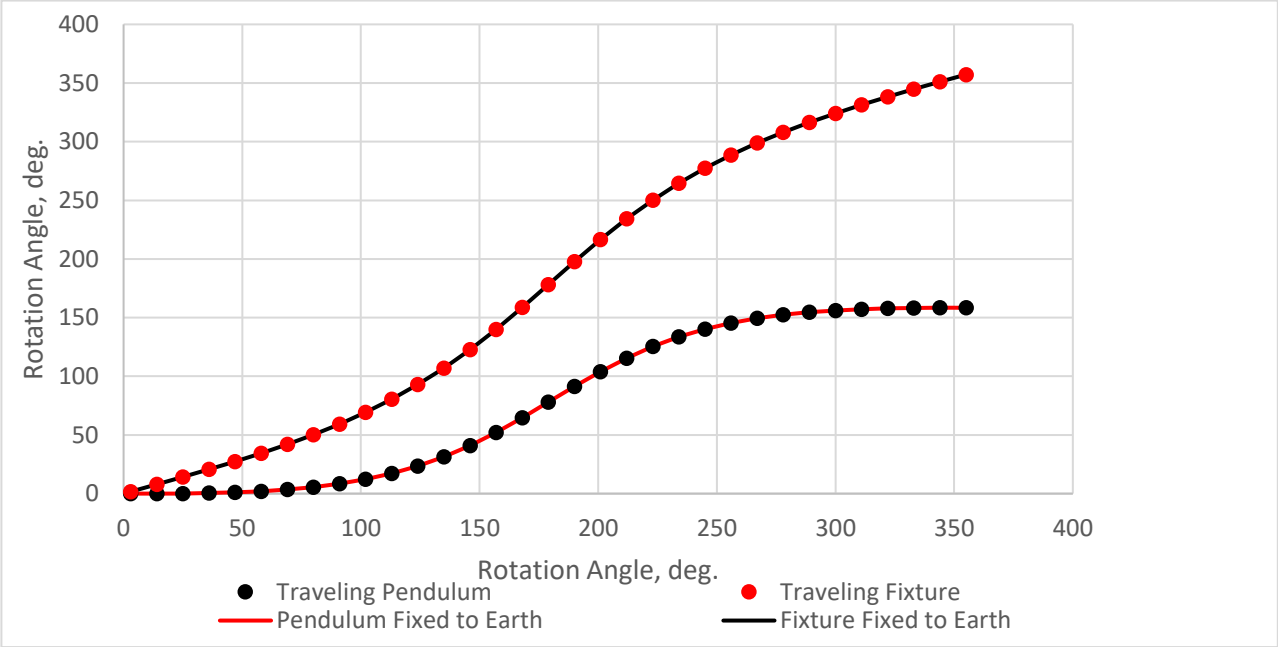

Fig. 24. Comparison of absolute rotations for spinning Earth/stationary pendulum versus non-spinning Earth/traveling pendulum.

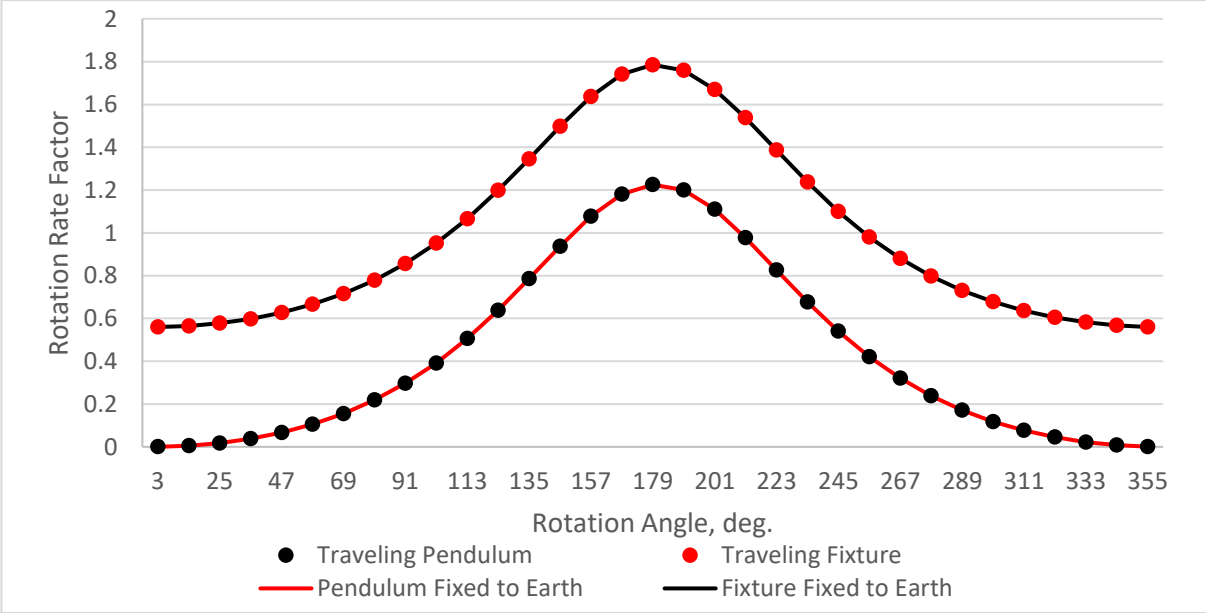

Fig. 25. Rotation rate factors for Fig. 24.

6. Conclusion

The analytical equation for the absolute rotation of the Foucault Pendulum about its vertical axis for arbitrary Earth rotation angle and latitude was derived. The rotation angle was found to be the solid angle enclosed by the actual trajectory of the vertical axis and the great circle arc trajectory linking the initial and final orientations of the axis. A new method to obtain the solid angle enabled the derivation of an analytical solution. A similar equation was derived for the pendulum's MF; however, the MF also includes a rotation given by the time integral of the Earth's rotation rate along the pendulum's vertical axis. It was found that every complete rotation of the Earth causes the MF to rotate once about its vertical axis for any latitude location. Using the derivatives of the analytical equations, the rotation angle rate of both the pendulum and its MF were derived and found to be nonlinear functions of the Earth rotation angle. The difference in the rotation rates is in agreement with the rate of precession of the Foucault Pendulum when observed in the local reference frame.

A method to compute the absolute rotation of a traveling pendulum was developed using a rotation about an auxiliary Earth fixed axis to drive the pendulum motion across the Earth's curved surface. The absolute rotation of the pendulum's vertical axis was computed numerically for both great circle arc and conical arc trajectories connecting initial and final pendulum locations. For each trajectory, the absolute rotation of the MF was computed, as well as, the pendulum precession rate. It was shown that a traveling pendulum's vertical axis can have an absolute rotation even if the Earth's angular rate is zero. The method developed can be used to compute the absolute rotation for cases involving arbitrary Earth spin rate and arbitrary pendulum motion across the surface of the Earth.

This work demonstrates that the absolute rotation and precession rate of a stationary or traveling Foucault Pendulum can be determined using attitude kinematics without solving for the detailed oscillatory motion of the pendulum bob itself. Therefore, dynamic analysis is completely avoided using this method. It is likely that the methods developed in this work will be of use in solving related problems in the future.

References

Basano, L. A., 2018. "The Foucault Pendulum Precession and the Additivity of Infinitesimal Rotations," European Journal of Physics. (arXiv:1801.06101)

Bergmannn, J. V., Bergmann, H, V., 2007. "Foucault Pendulum through Basic Geometry," Am. J. Phys. 75 _10_, October.

Ciureanu, I. A., Condurache, D., 2015. "A short Vector Solution of the Foucault Pendulum Problem," World Journal of Mechanics, Vol. 5, 7-19. http://dx.doi.org/10.4236/wjm.2015.52002

Ishlinskii, A., Y., 1952. "The Mechanics of Special Gyroscopic Systems," Izd., Akrad. Nauk, UkrSSR, Kiev.

Oprea, J., 1995. "Geometry and the Foucault Pendulum," The American Mathematical Monthly, Vol. 102, No. 6, 515-522.

Patera, R. P., 2021. "Kinematics of the Foucault Pendulum," viXra: 2101.0150 (2021).

Patera, R. P., 2020a. “Attitude Kinematics using Slewing Transformation of a Single Axis,” Advances in Space Research 66, 1460-1474.

Patera, R. P., 2020b. “General Method of Solid Angle Calculation Using Attitude Kinematics,” viXra: 2008.0076.

Patera, R. P., 2017. “New Fundamental Parameters for Attitude Representation,” Advances in Space Research 60, 557-570.

Sommeria, J., 2017. “Foucault and the Rotation of the Earth,” Comptes Rendus Physique, Vol. 18, 520-525.

Zheng, Z., 2015. “Analysis on the Foucault Pendulum by De Alembert Principle and Numerical Simulation,” arXiv:1504.03873.

Zhuravlev, V. F., Petrov, A. G., 2014. “The Lagrange Top and the Foucault Pendulum in Observed Variables,” Doklady Physics, Vol. 59, No. 1, pp. 35–39.